

Radiative Muon Capture on Hydrogen and the Induced Pseudoscalar Coupling

G. Jonkmans,^{4*} S. Ahmad,^{1†} D. S. Armstrong,⁵ G. Azuelos,^{3,4} W. Bertl,⁷ M. Blecher,² C. Q. Chen,¹ P. Depommier,⁴ B. C. Doyle,^{1,6} T. von Egidy,^{3‡} T. P. Gorringer,⁶ P. Gumplinger,¹ M. D. Hasinoff,¹ D. Healey,³ A. J. Larabee,^{1§} J. A. Macdonald,³ S. C. McDonald,⁸ M. Munro,⁸ J.-M. Poutissou,³ R. Poutissou,³ B. C. Robertson,⁹ D. G. Sample,¹ E. Saettler,¹ C. M. Sigler,² G. N. Taylor,⁸ D. H. Wright,^{1,3} and N. S. Zhang,¹

(1) *University of British Columbia, Vancouver, B. C., Canada V6T 1Z1*

(2) *Virginia Polytechnic Institute and State University, Blacksburg, VA 24061*

(3) *TRIUMF, 4004 Wesbrook Mall, Vancouver, British Columbia, Canada V6T 2A3*

(4) *Université de Montréal, Montréal, P.Q., Canada H3C 3J7*

(5) *College of William and Mary, Williamsburg, VA 23187*

(6) *University of Kentucky, Lexington, KY 40506*

(7) *Paul Scherrer Institut, CH-5232 Villigen, Switzerland*

(8) *University of Melbourne, Parkville, Victoria, Australia 3052*

(9) *Queen's University, Kingston, Ontario, Canada K7L 3N6*

(October 12, 2018)

Abstract

The first measurement of the elementary process $\mu^-p \rightarrow \nu_\mu n \gamma$ is reported. A photon pair spectrometer was used to measure the partial branching ratio $(2.10 \pm 0.22) \times 10^{-8}$ for photons of $k > 60$ MeV. The value of the weak pseudoscalar coupling constant determined from the partial branching ratio is $g_p(q^2 = -0.88m_\mu^2) = (9.8 \pm 0.7 \pm 0.3) \cdot g_a(0)$, where the first error is the quadrature sum of statistical and systematic uncertainties and the second

error is due to the uncertainty in λ_{op} , the decay rate of the ortho to para $p\mu p$ molecule. This value of g_p is ~ 1.5 times the prediction of PCAC and pion-pole dominance.

23.40.-s, 13.10.+q, 23.40.Bw, 11.40.Ha

In semi-leptonic weak interactions the strong force can, in general, induce four couplings in addition to the usual vector (g_v) and axial vector (g_a) couplings: weak magnetism (g_m), pseudoscalar (g_p), scalar (g_s), and tensor (g_t) [1]. G-parity invariance predicts null values for g_s and g_t , in agreement with experiment [1–3]. The CVC prediction for g_m [4] also agrees with experiment [5]. Theoretical calculations [6] of 3% precision are available for g_p , but no measurement approaching such accuracy has been reported.

It is difficult to measure g_p in beta decay because of the small value of the 4-momentum transfer, q . In muon capture the pseudoscalar coupling contribution is larger. Capture on the proton allows a reliable calculation since this case is free of nuclear structure uncertainties. Assuming partial conservation of the axial current (PCAC) and pion-pole dominance of the pseudoscalar coupling, g_p can be related to $g_a(0)$ [7]. In Fearing’s notation [8],

$$g_p(q^2) = 6.77g_a(0) \frac{(m_\pi^2 + 0.88m_\mu^2)}{(m_\pi^2 - q^2)}, \quad (1)$$

where m_π is the charged-pion mass and m_μ is the muon mass. In ordinary muon capture (OMC), $\mu^-p \rightarrow \nu_\mu n$, $q^2 = -0.88m_\mu^2$, which is far from the pion pole. Thus g_a dominates g_p and a rate measurement of 4% precision [9] yields a 40% uncertainty in g_p . Combining many different OMC results yields only 25% precision [9] for g_p .

In radiative muon capture (RMC), $\mu^-p \rightarrow \nu_\mu n\gamma$, q^2 can be much closer to the pion pole, since $q^2 = m_\mu^2$ at the maximum photon energy ($k \sim 100$ MeV). The g_p contribution to the RMC amplitude is then more than 3 times its contribution to the OMC amplitude. Offsetting this long known, promising sensitivity to g_p is the fact that, in hydrogen, the partial branching ratio is $\sim 10^{-8}$. Due to this small probability and the many potentially large background sources, no previous measurement has been attempted.

The experiment was performed using the M9A muon beam at the TRIUMF cyclotron. Negative muons at 63 MeV/ c were selected by an rf separator, counted by four beam scintillators, and stopped in a liquid hydrogen target. The μ^- stop rate was $\sim 6.5 \times 10^5 \text{s}^{-1}$ and the π^- contamination was $\pi/\mu \leq 2 \times 10^{-4}$. Photons emerging from the target were detected by $\gamma \rightarrow e^+e^-$ conversion in a cylindrical lead sheet and analyzed by tracking the e^+ and

e^- paths in cylindrical drift and wire chambers. An axial magnetic field allowed the determination of the photon energy from the curvature of the e^+ and e^- paths. Concentric segmented cylinders of plastic scintillators just inside the lead converter radius (the A , A' , and B rings), just outside the lead converter radius (the C ring), and just outside the drift chamber outer radius (the D ring) provided the photon trigger via the logic $\overline{A} \cdot \overline{A'} \cdot \overline{B} \cdot C \cdot D$. Lastly, two layers of plastic scintillators and drift chambers surrounding the magnet were used to identify cosmic-ray backgrounds. For more details on the experimental setup, see Ref. [10].

Even a small π^- contamination in the beam could give rise to a potentially dangerous background, since each π^- produces photons from the charge exchange or capture reactions:

$$\pi^- + p \rightarrow \pi^0 + n \quad (60.7\%), \quad (2)$$

$$\hookrightarrow \gamma + \gamma \quad (k \sim 55 - 83 \text{ MeV}),$$

$$\pi^- + p \rightarrow \gamma + n \quad (39.3\%, k \sim 129 \text{ MeV}). \quad (3)$$

Although these pion-induced photons were $\sim 10^4$ times more plentiful than RMC photons, they were prompt and could be vetoed by a timing cut. They were, however, useful for measurement of the acceptance and quantitative comparison to Monte Carlo modeling of the detector. For this measurement the beam was periodically tuned for 81 MeV/ c π^- , which stopped at the same place in the target as the 63 MeV/ c μ^- . The pion-induced photons were subjected to the same geometry cuts as were the photons from μ^-p , but not to the timing cuts. Excellent agreement with Monte Carlo was obtained [10], especially in the π^0 region which overlaps the RMC region, providing an energy calibration to ~ 0.25 MeV.

The spectrometer energy resolution, $\sim 11\%$ FWHM for photons, was sufficient to eliminate most of the background for $k > 60$ MeV from μ^- decay with internal or external bremsstrahlung, $\mu^- \rightarrow e^- \overline{\nu}_e \nu_\mu \gamma$. These photons have a maximum energy of $m_\mu/2$, which prevents study of RMC at lower energies. Furthermore, $\mu \rightarrow e \overline{\nu} \nu \gamma$ events could leak from the region $k < 60$ MeV into the region $k > 60$ MeV due to the high-energy tail of the spectrometer resolution function. To determine this high-energy tail background the photon

spectrum from μ^+ stops, where decay is present but capture is absent, was measured. Comparison of the normalized μ^+ and μ^- photon spectra, accounting for in-flight annihilation which contributes to the former but not the latter, yielded a $(17.2 \pm 2.5)\%$ high-energy tail background in the RMC spectrum.

Some fraction of the cosmic-ray induced events were not identified in the cosmic-ray detectors surrounding the spectrometer magnet, and thus survived the software veto. The residual background was measured under experimental conditions when the beam was off. This and any proton “beam related” background was measured when the secondary beam was diverted to other channels. The combined background photon energy spectrum, normalized by time and integrated proton current, agrees with the spectrum, $100 < k < 200$ MeV, produced by the μ^- beam. This energy range is above the RMC range and allowed a reliable extrapolation and subtraction of these backgrounds, $(10 \pm 4)\%$, in the RMC region.

Muon capture occurs on the Au flask containing the liquid H and on the surrounding Ag heat shields much more rapidly than on H. Au was chosen for the flask material because it can be made into a very pure thin-walled container. Also, the disappearance time for μ^- in Au is 73 ns, in Ag 89 ns, while in H it is 2195 ns [11]. Events which occurred within 365 ns ($5\tau_{Au}^{\mu^-}$) following the last μ^- stop were “blanked” in software. A fit to the unblanked time spectrum for $k > 60$ MeV enabled a determination of the part of this background which occurred more than 365 ns after a stop. The net background from the Au and Ag was $(10 \pm 4)\%$.

Impurities of deuterium or heavy elements in the liquid hydrogen could have been a serious source of backgrounds. In liquid the μ^- is rapidly captured into the singlet atomic state. This small neutral system quickly forms a $p\mu p$ molecule, usually in the ortho state, which can decay ($\lambda_{op} = (4.1 \pm 1.4) \times 10^4 \text{s}^{-1}$ [9]) to the para state. However, if there are contaminants the μ^- can transfer from the proton to form a μA atom. Heavy impurities were reduced to $\ll 10^{-9}$ by thorough bakeout and pumping, and by passing the gas through a palladium filter [12]. If deuterium is present a μd atom can be formed, followed by a $p\mu d$ molecule. The latter can form a $\mu^3\text{He}$ system via muon-induced fusion. Natural H contains

> 100 ppm deuterium, and since capture on ${}^3\text{He}$ occurs at a much higher rate than on H, the background from ${}^3\text{He}$ RMC would be larger than the H signal. Our liquid was obtained from the electrolysis of two samples of deuterium-depleted H_2O . For half of the data-taking it contained 1.4 ± 0.2 ppm deuterium [13], while for the other half this contamination was < 0.1 ppm. A $(1.1 \pm 0.3)\%$ ${}^3\text{He}$ RMC background was determined from a short run with natural H.

Other background sources were explored. These include: 1) π^- and μ^- capture in the Pb beam collimators without hits in the beam counters. As these collimators were located quite far from the target such events were vetoed by geometry cuts. 2) Beam π^- could decay in flight to high-energy μ^- which would capture on the Au/Cu backplate of the target. The beam simulation which reproduced the observed stopping distribution indicated that the number of such events was small and a geometry cut further reduced them. 3) μ^- which stopped in the veto scintillators would capture on C which has a disappearance time similar to H. The stopping simulation indicated this background was $< 1\%$. 4) Before forming a $p\mu p$ molecule the μp atom could diffuse into the Au and capture after a long time, thereby defeating the blank cut. The beam simulation showed very few stops within 2 mm of the Au flask. The mean free path of such atoms is $\ll 1$ mm and thus this background is negligible. 5) Multiple single tracks in near-coincidence could imitate high-energy pairs. However, all trigger counters were connected to multihit TDCs, which allowed a straightforward veto of these spurious events. The net contribution from all these background sources was $(3 \pm 2)\%$.

Data taking took place over a 3.5 year period. The total number of μ^- stops examined was 3.6×10^{12} . The uncut photon energy spectrum is shown in Fig. 1. The peaks are from bremsstrahlung and pion-induced reactions. The shaded region shows the spectrum after application of the prompt cut, indicating elimination of pion events. The number of RMC photons observed ($k > 60$ MeV), after all cuts and background subtractions, is $N_0 = 279 \pm 26$.

The open histogram in Fig. 2 shows the photon spectrum after geometry, timing, cosmic ray, and energy ($k > 60$ MeV) cuts were imposed. The overlaid dark shaded region shows

the remaining bremsstrahlung background, obtained from the normalized μ^+ spectrum (with annihilation-in-flight removed). The light shaded region shows the photon spectrum after the residual Au, Ag, ^3He , cosmic ray, “beam-related” and bremsstrahlung backgrounds have been removed. This represents the first observation of a signal from RMC on hydrogen.

In order to extract g_p from the data, a calculation of the RMC branching ratio R_γ and photon energy spectrum in terms of g_p was made using the theory of Fearing and Beder [14]. This is a relativistic approach based on tree-level Feynman diagrams. Monte Carlo events were generated from the theoretical photon spectrum for $k > 50$ MeV, $t > 365$ ns, and several values of g_p , and then analyzed like experimental events. The q^2 dependence of g_p assumed was that of Eq. 1. The values of the partial branching ratio and g_p were obtained when the number of Monte Carlo RMC events N was equal to the number of experimental RMC events N_0 .

The number of Monte Carlo events generated was

$$N = R_\gamma \kappa N_\mu \epsilon_{cr} P F_a. \quad (4)$$

N_μ is the number of beam counter coincidences (stops), corrected for multiple μ^- in a beam burst. ϵ_{cr} is the efficiency of cuts to eliminate multiple single particles and cosmics (these cuts were not applied to pion-induced photons from which the acceptance was obtained, nor to simulated photons). It is 0.93 ± 0.01 and was obtained by noting the effect of these cuts on μ^- beam events which were rejected by the prompt cut, i.e. π^- -induced events which came in the μ^- beam. Pileup muons blank a fraction $1 - P$ of real and background events which are captured more than 365 ns after a stop, where $P = 0.750 \pm 0.011$ was calculated from knowledge of the timing logic and the incident beam rate. This calculation reproduced the ratio of events before and after the blank cut, after all other cuts had been imposed. F_a is the ratio of the measured acceptance in each run period to the simulated acceptance. The acceptance was independent of beam rate and within a running period was constant to within a few percent, but there were variations of up to 10% between running periods.

The factor $\kappa = 0.88 \pm 0.01$ is a run-independent product of several small, measured or

calculated corrections. The largest, 0.926 ± 0.005 , is the fraction of muons in N_μ that stopped in the liquid. It was measured by replacing the liquid with a scintillator of appropriate shape and counting coincidences with the beam counters; the measured value agreed with Monte Carlo predictions of the beam. Other factors in κ , each of which had less than a 2% effect, included small measured inefficiencies in the beam and trigger counters, random vetoing in the trigger due to the singles rates in the A, A', B veto scintillators, and muon miscounting related to electrons in the beam or from the target.

Due to the spin-dependence of the weak interaction, the extraction of g_p from the data depends on knowledge of the relative fraction of muons in the ortho and para $p\mu p$ states. Thus the Monte Carlo, which includes all the muonic atomic and molecular processes, was run for various values of λ_{op} . The sensitivity to the rates of the other atomic and molecular processes was negligible.

Our measured partial branching ratio for photons of $k > 60$ MeV is $(2.10 \pm 0.20 \pm 0.09) \times 10^{-8}$, where the first error is statistical and the second systematic. This branching ratio arises from the mixture of muonic states relevant in the experimental time window ($t > 365$ ns): 6.1% in the singlet μp state, 85.4% in the ortho $p\mu p$ state and 8.5% in the para $p\mu p$ state. The shape of the energy spectrum in the experimentally-accessible region is in good agreement with the theoretical prediction (see Fig. 2). The results for g_p are shown in Fig. 3, where g_p/g_a is plotted versus λ_{op} . The expected theoretical result (Eq. 1) is $6.77 \cdot g_a(0)$, at $q^2 = -0.88m_\mu^2$. RMC yields $g_p/g_a(0) = 9.8 \pm 0.7 \pm 0.3$, a factor ~ 1.5 times the expected value, if the experimental value $\lambda_{op} = (4.1 \pm 1.4) \times 10^4 \text{s}^{-1}$ [9] is used. The first error includes statistical and systematic errors added in quadrature, while the second is due to the error in λ_{op} . The present result for g_p is independent of energy cut, $k > 60$ MeV, blank time cut, $t_b > 365$ ns, and is not very sensitive to λ_{op} .

In Fig. 3, “Saclay” refers to the most recent and accurate OMC measurement [9], while “World” refers to the world average of OMC (including older bubble chamber) data [9]. It should be noted that this average was obtained from many different experiments with widely varying conditions and results. Within large errors, OMC is in agreement with the

expected value of g_p if one adopts the measured value of λ_{op} . However, the OMC results are generally more sensitive to λ_{op} than the present measurement, especially the “Saclay” result, and the extracted value of g_p would decrease significantly if the theoretical value $\lambda_{op} = (7.1 \pm 1.2) \times 10^4 \text{s}^{-1}$ [15] is correct.

In conclusion, we have made the first measurement of the elementary radiative muon capture process, and determined a partial branching ratio of $(2.10 \pm 0.22) \times 10^{-8}$, for photons of $k > 60$ MeV. We have assumed that the measured values of λ_{op} and other μH parameters are correct, the q^2 dependence of g_p is given by (1), the R_γ and energy spectrum for RMC on H are correctly predicted by a relativistic perturbation theory calculation [14] based on tree-level Feynman diagrams, and that a large background has not eluded detection in this experiment. Based on these assumptions, a substantial deviation of g_p from the predicted value is obtained.

We wish to thank the TRIUMF hydrogen target group, in particular A. Morgan and P. Burrill for their excellent work on our target. We are grateful to H. Fearing for access to his RMC computer code and helpful discussions. This experiment was supported by the NSERC and NRC of Canada, the NSF of the USA, the PSI of Switzerland, and the ARC of Australia.

REFERENCES

- * Present address: Queen's University, Kingston, ON, Canada, K7L 3N6.
- † Present address: Rice University, Houston, TX, 77251.
- ‡ Sabbatical visitor from Technische Universität München, D-85748, Garching, Germany.
- § Present address: University of Texas, El Paso, TX, 79968.
- [1] L. Grenacs, *Ann. Rev. Nucl. Part. Sci.* **35**, 455 (1985).
- [2] M. Morita, R. Morita, and K. Koshigiri, *Nucl. Phys.* **A577**, 387c (1994)
- [3] P. Baringer *et al.*, *Phys. Rev. Lett.* **59**, 1993 (1987).
- [4] M. Gell-Mann, *Phys. Rev.* **111**, 362 (1958).
- [5] Y. K. Lee, L. Mo, and C. S. Wu, *Phys. Rev. Lett.* **10**, 253 (1963).
- [6] V. Bernard, N. Kaiser, and Ulf-G. Meissner, *Phys. Rev. D* **50**, 6899 (1994).
- [7] M. L. Goldberger and S. B. Treiman, *Phys. Rev.* **111**, 354 (1958).
- [8] H. W. Fearing, *Phys. Rev. C* **21**, 1951 (1980).
- [9] G. Bardin *et al.*, *Phys. Lett.* **B104**, 320 (1981) and references therein; G. Bardin *et al.*, *Nucl. Phys.* **A352**, 365 (1981); G. Bardin, Ph.D. thesis, U. de Paris-Sud(Orsay), 1982.
- [10] D. H. Wright *et al.*, *Nucl. Instrum. Methods* **A320**, 249 (1992).
- [11] T. Suzuki, D. F. Measday, and J. P. Roalsvig, *Phys. Rev. C* **35**, 2212 (1987).
- [12] W. Bertl *et al.*, *Nucl. Instrum. Methods* **A355**, 230 (1995).
- [13] Dept. of Earth Sciences, Univ. of Waterloo, Waterloo, Ontario, Canada N2L 3G1 and Metabolic Systems Inc., Acton, MA, USA 01720.
- [14] D. S. Beder and H. W. Fearing, *Phys. Rev. D* **39**, 3493 (1989).

- [15] D. D. Bakalov *et al.*, Nucl. Phys. **A384**, 302 (1982); L. Ponomarev, in *Muonic Atoms and Molecules*, L. A. Schaller and C. Petitjean eds., Birkhauser Verlag, 1993.

FIGURES

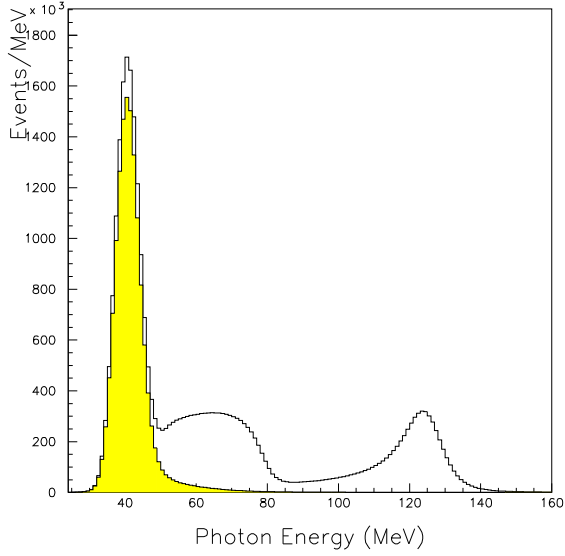


FIG. 1. Photon energy spectrum before cuts are applied; both μ^- and π^- induced events are observed. Shaded region: prompt cuts applied, pion events are eliminated.

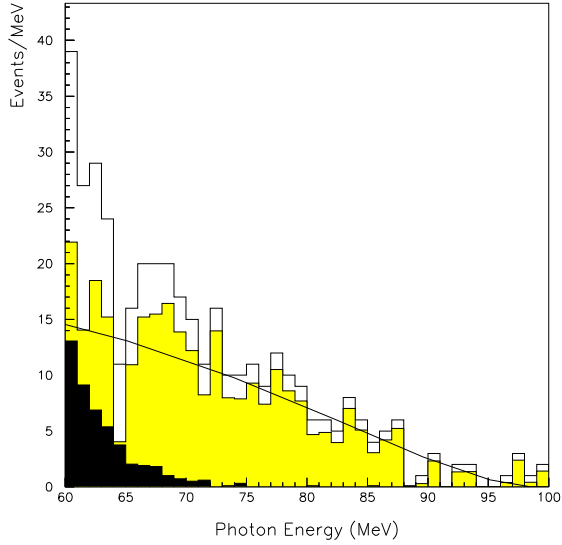


FIG. 2. Open histogram: Photon energy spectrum after all cuts were applied. Shaded histogram: final spectrum after background subtraction. Dark shaded overlay: normalized μ^+ (annihilation-in-flight removed) bremsstrahlung background spectrum. Curve: theoretical spectrum [14] for the best-fit value of g_p/g_a .

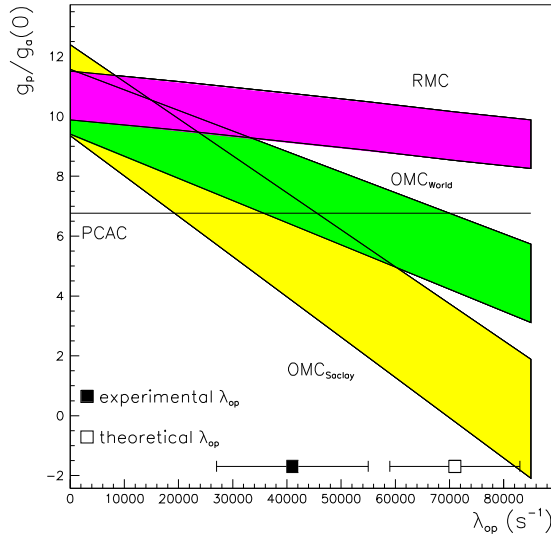


FIG. 3. $g_p(q^2)/g_a(0)$, evaluated at $q^2 = -0.88m_\mu^2$, vs. the ortho to para transition rate λ_{op} for OMC and RMC on hydrogen (see discussion in text).